Current Applied Physics 9 (2009) 598–604

Contents lists available at ScienceDirect

Current Applied Physics

journal homepage: www.elsevier.com/locate/cap

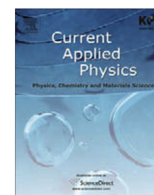

Effects of process parameters on the properties of silicon oxide films using plasma enhanced chemical vapor deposition with tetramethoxysilane

T.H. Chung *, M.S. Kang, C.J. Chung, Y. Kim

Department of Physics, Dong-A University, 840 Hadan-dong, Saha-Gu, Busan 604-714, Republic of Korea

ARTICLE INFO

Article history:
Received 1 February 2008
Received in revised form 23 April 2008
Accepted 9 May 2008
Available online 24 May 2008

PACS:
52.75.Rx
52.25.−b
73.90.+f

Keywords:
Silicon oxide thin film
Nitrogen-incorporated silicon oxide thin films
Plasma enhanced chemical vapor deposition
Tetramethoxysilane
Optical emission spectroscopy

ABSTRACT

Thin oxide films are deposited from tetramethoxysilane (TMOS) with some addition of O_2 (or N_2O) gas in inductively coupled plasma (ICP) discharges supplied with radio frequency power. The effects of various deposition parameters such as O_2 (or N_2O) partial pressure ratio, ICP power, and gas pressure on the growth characteristics and properties of the deposited films are investigated. The chemical bonding states of deposited films are analyzed by Fourier transform infrared spectroscopy, and the deposition rate and optical properties are determined from in-situ ellipsometry. For the TMOS/O_2 case, the deposition rate increases with increasing ICP power. Larger oxygen partial pressure ratio decreases the deposition rate. For the TMOS/N_2O case, higher N_2O fraction results in a decrease in nitrogen content in the gas-phase and in the deposited films, thereby decreasing the refractive index. As the gas pressure increases, the deposition rate increases first and saturates later. Capacitance–voltage measurements are performed in MOS capacitors to obtain the electrical properties of the deposited films. The interface trap density is observed to decrease with increasing ICP power.

© 2008 Elsevier B.V. All rights reserved.

1. Introduction

Silicon dioxide is one of the most widely used thin films as interlayer dielectric in integrated circuits and microelectronics devices. When the substrate materials have poor heat resistance, it is necessary to deposit silicon oxide at low temperature. Plasma enhanced chemical vapor deposition (PECVD) allows deposition of good-quality films at low substrate temperature.

Although silane has been widely employed as a silicon precursor, organosilicon sources such as TMOS (tetramethoxysilane: $Si(OCH_3)_4$) [1], TEOS (tetraethoxysilane) [2], TMS (tetramethylsilane) [3], HMDS (hexamethyldisilazane) [4], and HMDSO (hexamethyldisiloxane) [5] deposited with an oxidizer such as oxygen are used increasingly because they result in the conformal thin films and allow the deposition of a large variety of materials. Using low TEOS/O_2 flow ratio, high quality films could be deposited by PECVD at room temperature [6]. PECVD of silicon dioxide from organosilicon sources and oxygen plasma has been extensively investigated [1–10]. The primary issues have been how process conditions such as silicon precursor dilution, pressure, and power govern the deposition mechanism and the composition and properties of the deposited films.

In previous papers [11,12], we confined our efforts to finding some advantages of TMOS as a precursor for good-quality silicon oxide films over other precursors such as TEOS, HMDSO, or silane gas. We investigated the effects of parameters such as source RF power, substrate bias power, oxygen partial pressure, and total pressure on the deposition rate and on the chemical bonding states of SiO_2 thin films deposited from TMOS/O_2 in an inductively coupled RF plasma. The plasma was also characterized by using Langmuir probe and optical emission spectroscopy, and the correlation between the film properties and the plasma characteristics were explained [11].

Recently, nitrogen-incorporated silicon oxide thin films have attracted attentions since they are good candidates for gate dielectric material and for optical waveguides for micromechanical systems. Our study has been extended to nitrogen-incorporated silicon oxide thin films deposited by PECVD from the gas mixture of TMOS/N_2O [13,14].

In this study, we report some improvements in the deposition of silicon oxide films utilizing the mixtures of TMOS/O_2 or TMOS/N_2O. In particular, we investigate in detail the effects of various deposition parameters such as partial pressure ratio of O_2 (or N_2O), source RF power, and gas pressure on the deposition rate and the properties

* Corresponding author.
E-mail address: thchung@dau.ac.kr (T.H. Chung).

1567-1739/$ - see front matter © 2008 Elsevier B.V. All rights reserved.
doi:10.1016/j.cap.2008.05.011

of the deposited films. The optical properties of the deposited films are characterized by the refractive index measurements using in-situ ellipsomety. The characterization of the SiO_2 layers are also performed by ex-situ Fourier transform infrared spectroscopy (FTIR). In this study, optical emission spectroscopy (OES) is used to investigate the gas-phase chemistry in the deposition process. The precursor decomposition produces a larger number of atoms and simple molecules which contribute significantly to the determination of film properties [15]. The intensities of light emission from molecules and radicals in the plasma are measured by OES. Especially, the variation of the light intensities from N and C atoms with varying N_2O fraction is examined to correlate with film property. The electrical properties of the silicon dioxide film and SiO_2/Si interface are investigated using capacitance–voltage (C–V) measurements.

2. Experiment

The PECVD reactor utilizes an inductively coupled plasma (ICP) source operating at 13.56 MHz to sustain low-pressure (1–50 mTorr) high-density plasmas. The inductively coupled plasma yields a high degree of ionization and significant decomposition of the precursor. The gas flow of TMOS, O_2, and N_2O, regulated by mass flow controllers (AFC 50), are introduced downstream from the plasma about 10 cm above the substrate. Films are deposited on p-type Si (1 0 0) substrate at room temperature.

The plasma chamber consists of a stainless-steel cylinder with 28 cm diameter and 34 cm length. A 1.9-cm-thick by 27-cm-diam tempered glass plate mounted on one end separates the planar one-turn induction coil from the plasma. The induction coil is made of copper (with water-cooling) and connected to an L-type capacitive matching network and a RF power generator (ENI OEM-12). To control the ion bombardment energy, the electrode on which the substrate is placed can be independently driven by a capacitively coupled RF source. Hence independent control of the ion/radical flux (through the ICP power) and the ion bombardment energy (through the substrate bias power) is possible.

The partial pressures of the organosilicon compound (TMOS) and O_2 (or N_2O) are controlled by mass flow controllers. The total pressure is fixed at 10 mTorr if not otherwise mentioned. The ICP power is varied from 100 to 500 W (1000 W for the TMOS/N_2O case) and the substrate bias power is not applied. Deposition studies are carried out as functions of ICP power, gas pressure, and partial pressure ratios of O_2 (or N_2O). The ellipsometry measurements using the in-situ ellipsometer (Elli-situ 2000, Ellipso Tech) operating at He–Ne laser wavelength (632.8 nm) are performed to obtain the thickness and refractive index of the films. Incidence and outlet angles both are 70°. The deposition rate is determined from the ratio of the film thickness to the deposition time. The chemical bonding states of deposited films are analyzed by FTIR (BIO RAD Excalibur). The light intensities of emissive molecules and radicals in the plasma are collected by an optical fiber, that is coupled to multi-channel spectrometer (OPC-2000, Optel-Precision). Light emission from glow discharge is detected through a home-made optical probe during deposition in the wavelength range of 300–900 nm with a resolution of 1 nm. The dependence of the emission intensities on the process parameters is investigated. High frequency capacitance–voltage (C–V) measurements are performed using a probe connected to a computer controlled capacitance-meter (Keithley 590). The C–V samples are prepared in the way that thermally evaporated Al is used for the Si back electrode and as the capacitor electrode.

3. Results and discussion

Fig. 1a shows the thickness of the films during the deposition time of 5 min as functions of O_2 partial pressure ratio and applied ICP power for the TMOS/O_2 case. The pressure is kept constant at 10 mTorr. As the O_2 partial pressure ratio increases, the deposition rate decreases.

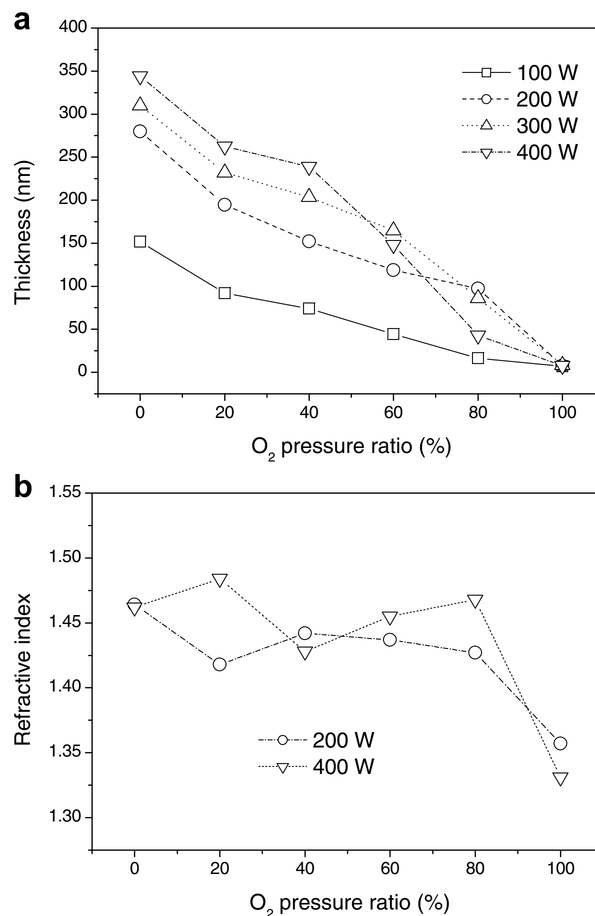

Fig. 1. (a) Thickness of the films during the deposition time of 5 min versus O_2 partial pressure ratio for different applied ICP powers, (b) refractive index versus O_2 partial pressure ratio for different applied ICP powers.

It has been known that either electron impact processes or atomic oxygen processes control the deposition rate [1,6,7]. As the O_2 partial pressure ratio increases, the frequencies of the electron impact dissociation of TMOS and its reaction with atomic oxygen are decreased. It has been established that electrons have a key role in TEOS fragmentation while the contribution of O is shown to be very weak [16]. The films are etched by O atoms. The etching rate is proportional to the density of O atom and is of the same order of magnitude as the deposition rate, which demonstrates that deposition and etching really compete in O_2/TEOS plasma [16].

The deposition mechanism from TMOS can be explained in a similar fashion to that from TEOS. The TMOS molecules are almost completely broken into small radicals in the plasma [7,8]. The Si–O–Si network is formed from the surface reactions of these fragments. The deposition occurs through an ion-assisted and an oxygen atom initiated pathways [17]. The deposition rate depends on a sum of oxygen atom induced and oxygen ion-assisted pathways.

Starting from the TMOS only case (O_2 partial pressure ratio = 0), the film thickness (thus deposition rate) decreases with increasing oxygen partial pressure ratio. The role of oxygen atom is generally assumed to be involved in TMOS dissociation in the gas-phase and to be responsible for the elimination (etching) of C and H atoms from the growing films [18].

In the case of high O_2 partial pressure ratio, the deposition rate is limited by the availability of TMOS and the etching reaction of O

atoms, while in the case of low O_2 partial pressure ratio, the surface is covered with the fragments of TMOS and the deposition rate is limited by the availability of O atoms. A similar trend is found in the case of HMDSO where the deposition rate depends linearly on the HMDSO concentration [19]. Note that deposition rate achieved in this study is comparable to that obtained in microwave plasma reactors [20].

The maximum deposition rate of SiO_2 is about 700 Å/min, quite high for room temperature depositions. The figure also indicates the effect of ICP power on the deposition rate. As the applied ICP power increases, the deposition rate increases since the frequency of the electron impact dissociation of TMOS is increased. A linear increase in the deposition rate with increasing ICP power is observed except at the higher O_2 pressure ratios of 60% and 80%. This may be explained by the increase in the active reaction species due to high dissociation frequency [21].

Fig. 1b shows the variation of refractive index of the deposited film for several values of O_2 partial pressure ratio and applied ICP power. It is observed that the refractive indices, which range from 1.34 to 1.50, do not have explicit dependence on the ICP power and O_2 partial pressure ratio. At the O_2 partial pressure ratio of 0.2, the refractive index is a little higher than that of thermal SiO_2 $n \simeq 1.456$). For lower oxygen fraction in the gas, the refractive index may increase due to incorporation of carbon species [22,23].

It was previously shown in different PECVD reactors that the refractive index decreased with increasing oxygen concentration at a fixed flow rate of precursor molecules [3,24]. The refractive index of a thin film depends on the composition, chemical bonding, and densification of the film in a very complex manner. In an inductively coupled CVD reactor, the ion bombardment on the film is determined by the difference between plasma and floating potential, which depends on the electron temperature. The electron temperature is not simply dependent on the applied ICP power, therefore, one should not expect an increase of densification of the films with the applied power [25]. Although the deposition rate is expected to increase with the applied power as seen in Fig. 1a, the effects of the ICP power on the refractive index do not exhibit such a consistent tendency. Generally speaking, the abundance of carbon, oxygen, and nitrogen atoms (and hydrogen atom sometimes) in the film contribute to the determination of the refractive index [3,26]. We can attribute the decrease of the refractive index to the incorporation of more oxygen in the film. The variation of refractive index of the deposited film with O_2 pressure ratio has a similar tendency to the results of our previous work on the deposition using the mixture of $TMOS/O_2$ [12]. But, more thorough analysis may be needed to give the physical explanations on the variation of refractive index.

Fig. 2 shows FTIR spectra of films deposited at various ICP powers and oxygen partial pressure ratios for the $TMOS/O_2$ case. The gas pressure is fixed at 10 mTorr. The spectra exhibit absorption peaks corresponding to Si–O–Si stretching at 1059 cm^{-1}, Si–O–Si deformation at 806 cm^{-1}, Si–OH stretching at 926 cm^{-1}. The spec-

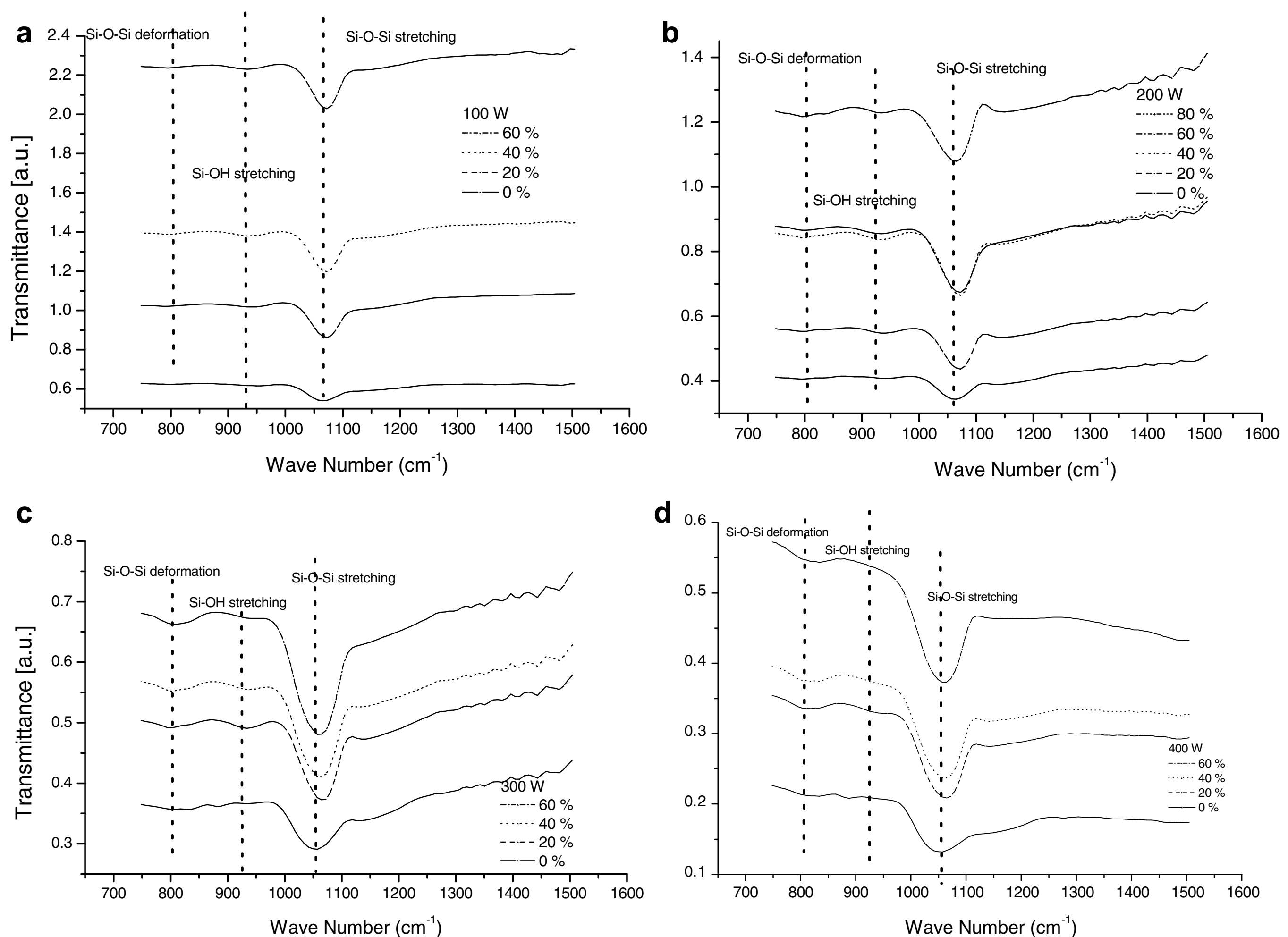

Fig. 2. FTIR transmission spectra for the films deposited at various oxygen partial pressure ratio and ICP power P_p: (a) $P_p = 100$ W, (b) $P_p = 200$ W, (c) $P_p = 300$ W, and (d) $P_p = 400$ W, $p = 10$ mTorr.

tra show a quite strong dependence on the ICP power and the oxygen partial pressure ratio. It is observed that as the ICP power is increased the Si–OH peak decreases. The OH elimination is achieved due to the temperature increase of the substrate at higher ICP power. As the oxygen partial pressure ratio is increased, the Si–O–Si peaks increases, and the Si–OH peak decreases. Thus, it can be stated that the density of the Si–O–Si bonding group increases with increasing ICP power and with increasing the oxygen partial pressure ratio. A similar trend was observed in our previous works [11,12] and in the O_2/TEOS case [27]. The remaining Si–OH bands in the deposited film are due to the low substrate temperature. This residual Si–OH bands reduces the electrical resistivity and degrade the mechanical properties.

Fig. 3 shows FTIR spectra of films deposited at various values of ICP power for the TMOS/N_2O case. The gas pressure is fixed at 10 mTorr. The samples are numbered from T1 (p_{TMOS}:p_{N_2O} = 1:9) to T9 (p_{TMOS}:p_{N_2O} = 9:1). The spectra were obtained from films with the same thickness (200 nm). The spectra exhibit absorption peaks corresponding to Si–O–Si stretching band at 1045–1075 cm^{-1}, Si–N stretching at 960 cm^{-1}, Si–O–Si bending at 810 cm^{-1}, Si–O–Si rocking mode at 460 cm^{-1} [28–30]. The broad peak at $1000-1100$ cm^{-1} corresponds not only to Si–O–Si, but also Si–O–C and even Si–C–Si [31]. The absorption band 850–1000 cm^{-1}, which can be attributed to the formation of nitrogen-incorporated oxide become dominant as the TMOS fraction increases (T7,T9). As the N_2O fraction decreases, the absorption bands at 1000–1100 cm^{-1} are broadened and shifted to lower wavenumbers (T7,T9) [32,33]. In addition, there are also Si–NH bending mode and Si–N bending mode evident at 1175 and 475 cm^{-1}, respectively. The peaks of Si–N bending and Si–NH bending modes indicates that the deposited films incorporate higher amount of nitrogen atoms at the ICP power of 500 W.

Fig. 4 shows the optical emission spectra of the TMOS/N_2O plasmas with various mixing ratios. The dominant peaks are N_2 molecular peaks (715.6, 442, 446, and 463 nm), C atom peak (578.8 nm), N atom peak (502.5 nm), CH (431 nm), C_2 (516 nm), N_2^+ (479 nm). H (433 nm) peaks. Besides, there are peaks of H (656 nm) which seems to be superposed to the emission due to the first positive system of nitrogen molecule and N_{II} (660 nm), N_V (671.8 nm), N_V (685–688 nm). Although not shown in the figure, it is found that all signal peaks in the spectra increase monotonically with an increase in the ICP power. This confirms that as the ICP power increases, the frequency of the electron impact dissociation of TMOS is increased.

The optical emission spectra exhibit quite a big difference from those for the TMOS/O_2 discharges in which the emission spectra is dominated by the emission lines due to H, OH, C_2, CH, O and O_2 [11]. With the addition of N_2O gas, the spectra exhibit characteristics typical to N_2 discharges. This tendency is significant especially for the higher N_2O fraction. The emission characteristics typical to N_2 discharges disappears with increasing the TMOS fraction. However, it should be noted that the emission from N atom (502.5 nm) gets larger with increasing the TMOS fraction.

Fig. 5a shows the evolution of the peak emission intensity of C (578.8 nm) and N_{II} (502.5 nm) from carbon and nitrogen atom as a function of the TMOS/N_2O pressure ratio. The parameter R is defined as the ratio of partial pressure of the TMOS gas to the N_2O gas (i.e. $R = p_{TMOS}/p_{N_2O}$). The N peak increases with R while the C peak exhibits insignificant change. Since the actinometry measurement is not performed in this work, it is difficult to assume that the intensity of the emitted light is proportional to the density of ground state species. However, the excitation cross sections and the threshold values of these atoms are not quite different, and thus it may be stated that the intensity of emitted light can provide some clue on the evolution of atomic abundance in the plasma.

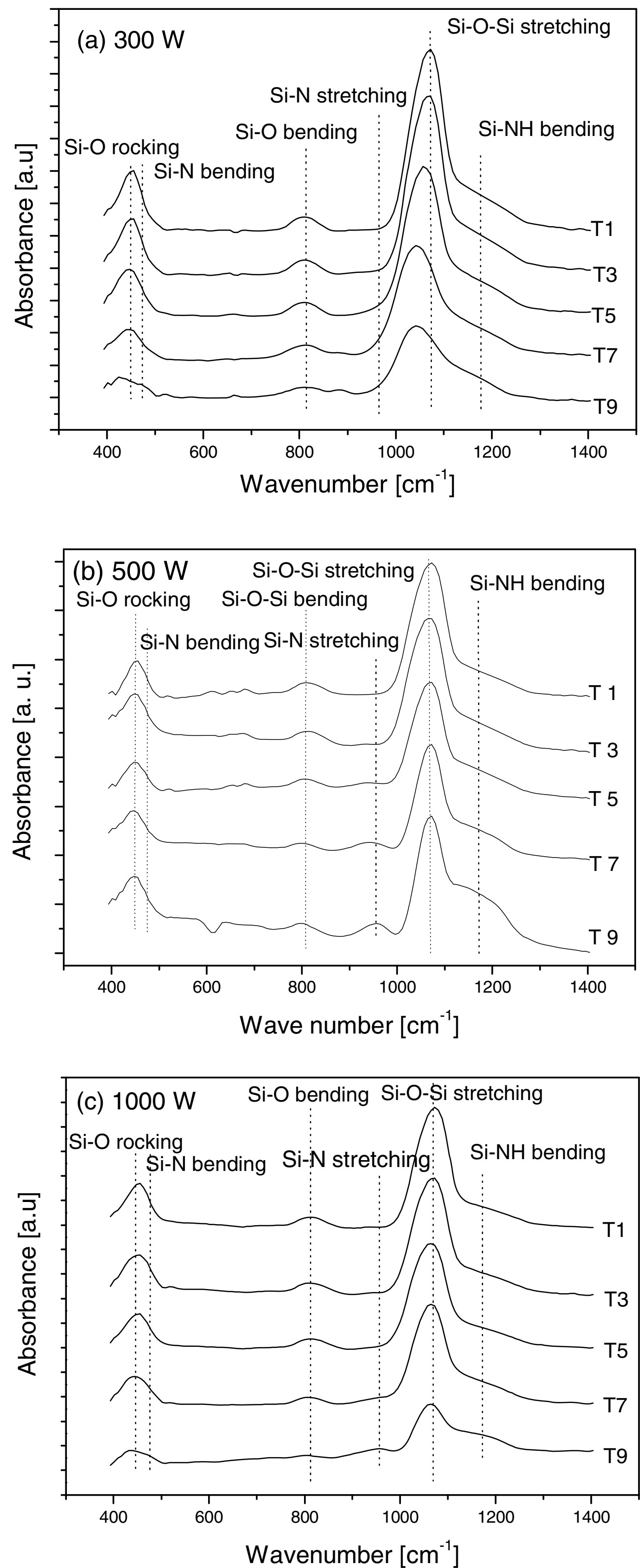

Fig. 3. FTIR spectra of the films deposited at various ICP powers for the TMOS/N_2O case: (a) $P_p = 300$ W, (b) $P_p = 500$ W, and (c) $P_p = 1000$ W.

In a previous study, [14], the composition of the films were estimated by using an X-ray photoelectron spectroscopy and the result is shown again in Fig. 5b. The atomic concentrations of N and C atoms in the film increase with R. The refractive index was found

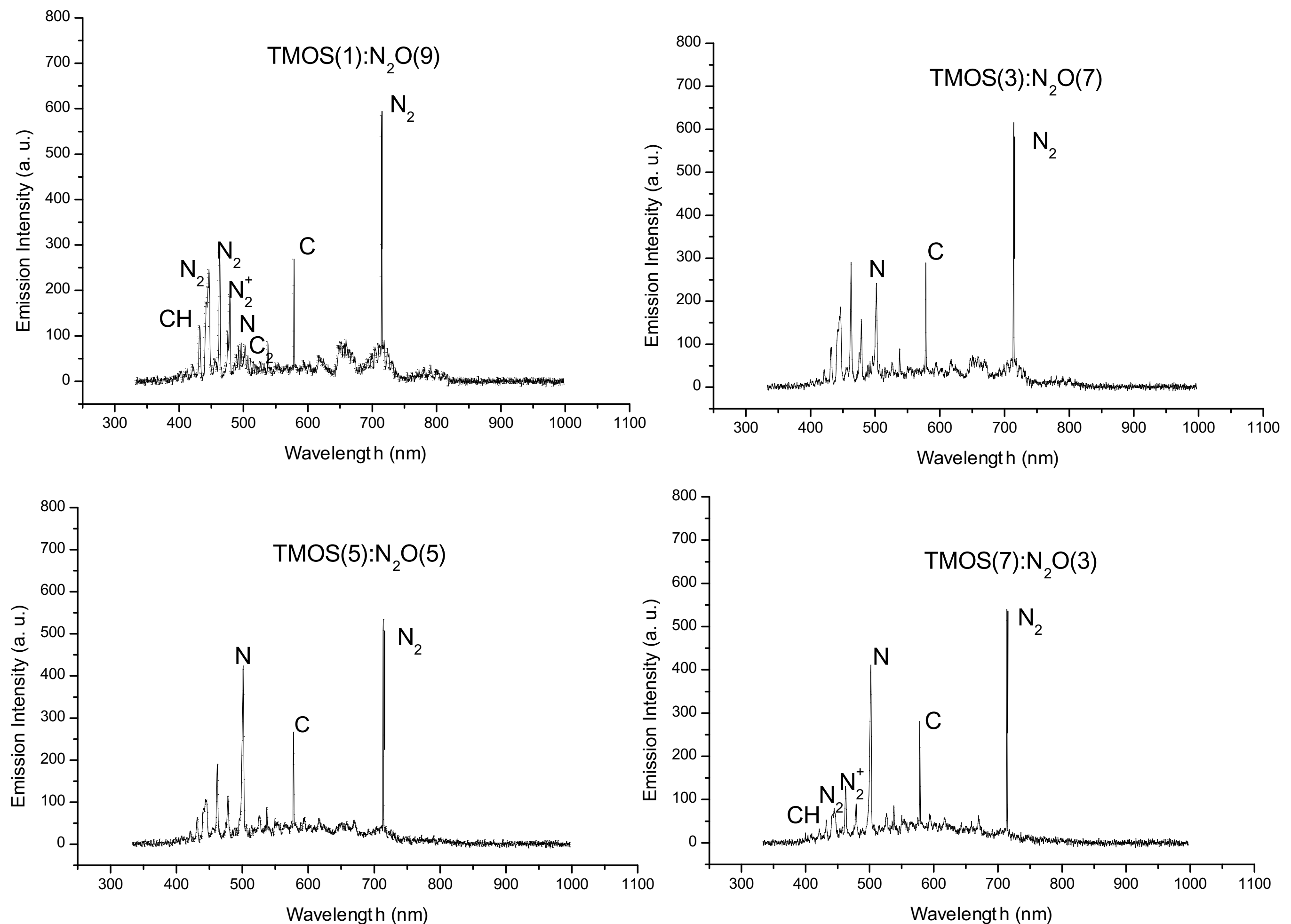

Fig. 4. Optical emission spectra of the TMOS/N_2O plasmas with various TMOS fractions, where $p = 10$ mTorr.

to increase with R [14]. Therefore, the increase in the N atom content contributes to the increase in the refractive index of the deposited film.

Fig. 6 shows the effect of pressure on the deposition rate and the refractive index of the deposited films. The deposition from the gas mixture of TMOS/N_2O is carried out at a pressure ratio of 8:2 and at the ICP power of 500 W. The pressure is varied from 7 to 15 mTorr. As the pressure increases, the deposition rate increases and saturates after reaching at a maximum of 840 Å/ min.

The deposition pressure determines the mean free path of electrons colliding with the gas molecules. As the gas pressure increases, the residence time of gases at the deposition surface increases and the deposition rate increases at the low-pressure region [34]. A recent modeling study of O_2/organosilicon gas performed by Yanguas-Gil et al. [35] indicates that the frequency of the electron impact process decrease with pressure, and the frequency of the reaction of precursor with atomic oxygen has a broad maximum at a specific value of pressure. This might be related to the behavior shown in Fig. 6.

A composite process parameter ϕ was formulated as [36]

$$\phi = \frac{WkT}{pMf}, \tag{1}$$

where W is the discharge power, T is the gas temperature, p is the total pressure, M is the monomer molecular mass, and f is the gas flow rate. At a certain value of ϕ, the conversion time has a minimum and the fragmentation rate has a maximum. At that point, the deposition rate has a maximum. This might be why the deposition rate has a maximum at a specific value of pressure in Fig. 6.

As can be seen in Fig. 6, the refractive index lies between 1.48 and 1.53. These values are little higher than that of thermal SiO_2. The refractive index increases with the gas pressure first, and then decreases again. As the pressure increases, the reactions $N_2O + O \rightarrow 2NO$, and $NO + O \rightarrow NO_2$ are expedited. This might cause the nitrogen composition in the film to decrease with a further increase of gas pressure, and the refractive index, which is proportional to the nitrogen content in the film, has a maximum at a specific value of pressure (here, $p = 10$ mTorr).

Fig. 7 shows the C–V curves of the silicon oxide films deposited from the TMOS/O_2 case at different ICP powers. In the previous work [12], it was observed that the fixed oxide charge density decreased with increasing the oxygen gas fraction and with increasing substrate bias power, while the interface trap density increased with increasing the oxygen gas fraction and with increasing substrate bias power. In this work, we investigate the effect of ICP power on the C–V characteristics of the deposited film. The C–V curves are shifted to negative voltage. A negative flat-band voltage (V_{fb}) indicates the presence of positive charges in the oxide. These positive charges are defects which are usually holes trapped at oxygen vacancies [37]. The V_{fb} becomes more negative gate voltage with increasing ICP power because increasing power leads to an increase in oxygen vacancy defects. The fixed charge density (Q_f) increases with increasing ICP power.

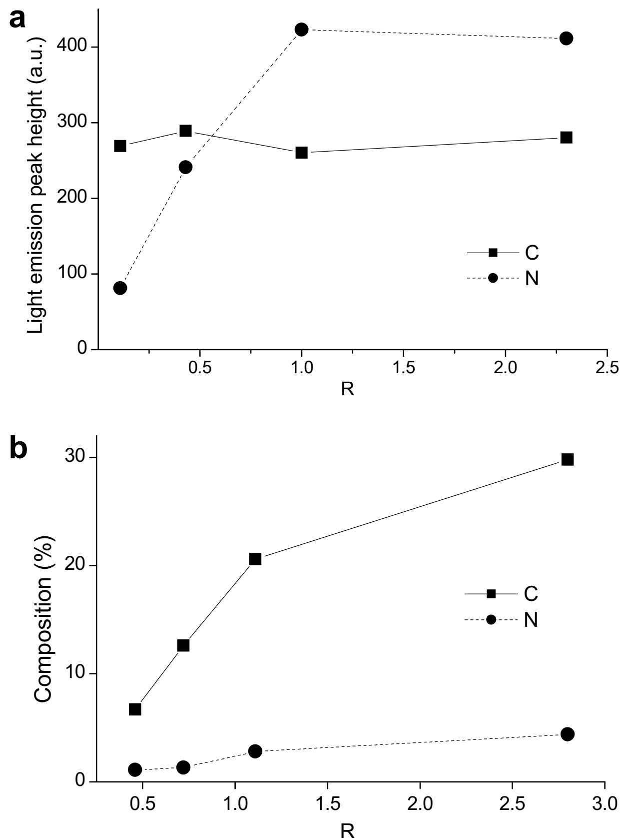

Fig. 5. (a) Variation of the optical emission intensities from N and C atoms as a function of TMOS and N_2O pressure ratio (R). (b) Variation of the atomic concentration of the elements in the deposited film as a function of R.

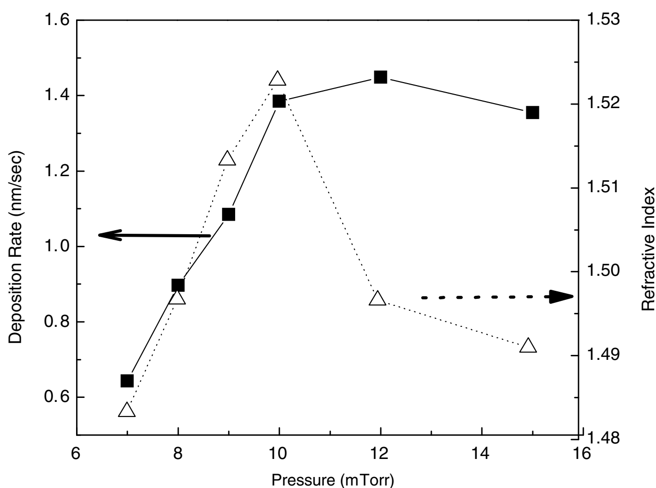

Fig. 6. Deposition rate and index of refraction as a function of pressure, where $P_p = 500$ W

Capacitance–voltage stretch out allows us the qualitative discussion about the variation of D_{it} depending on ICP power [38]. The slope of the C–V curves gradually increases with the decreasing ICP power, indicating the decrease in the interface trap density, D_{it} [39]. Therefore, the results indicate that defects and/or contaminants are increased by increasing ICP power.

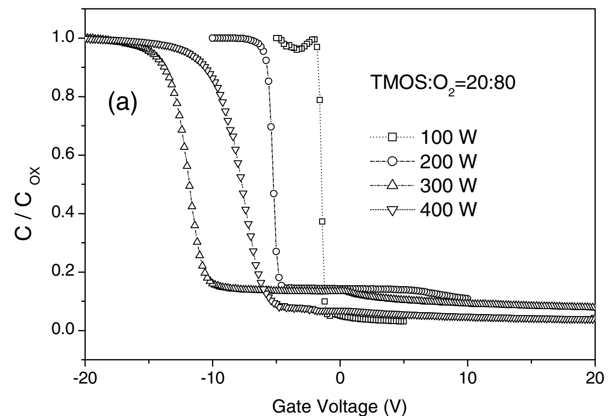

Fig. 7. C–V curves of the films deposited from the TMOS/O_2 at different ICP powers, where O_2 partial pressure ratio is 80% and $p = 10$ mTorr.

4. Conclusion

Plasma enhanced chemical vapor deposition of silicon dioxide thin films using TMOS and O_2 (or N_2O) was investigated in an inductively coupled RF discharge. The optical and electrical characteristics of the deposited films have been studied with varying process parameters. The process parameters such as partial pressure ratios of O_2 (or N_2O), applied ICP power, and gas pressure has profound effects on the deposition rate and the film properties. For the TMOS/O_2 mixture, the deposition rate increases with increasing ICP power and with decreasing the oxygen partial pressure ratio. The deposition rate of about 700 Å/ min is achieved, quite high for room temperature depositions. As the ICP power increases, the SiOH fraction in the films reduces due to an increase in the ion bombardment energy. From the C–V curves of the silicon oxide films, the interface trap density is observed to decrease with increasing ICP power. For the TMOS/N_2O mixture, the optical emission spectra indicate that the N peak increases with decreasing the N_2O fraction while the C peak exhibits insignificant change. The atomic composition and the refractive index of the deposited film measured in the previous study supports the variation of the gas-phase abundance of nitrogen atom with the TMOS fraction in the gas mixture. Since the refractive index was found to increase with increasing the TMOS fraction (decreasing the N_2O fraction), it may be stated that the increase in the N atom content in the deposited film contributes to the increase in the refractive index. As the pressure increases, the deposition rate increases and saturates after reaching at a maximum value of 840 Å/ min. The refractive index increases first and then decreases again with increasing pressure.

Acknowledgement

This work was supported by the research fund of Dong-A university.

References

[1] Y. Inoue, O. Takai, Plasma Sources Sci. Technol. 5 (1996) 339.
[2] K. Aumaille, C. Vallee, A. Granier, A. Goullet, F. Grolleau, G. Turban, Thin Solid Films 359 (2000) 188.
[3] A. Grill, V. Patel, J. Appl. Phys. 85 (1999) 3314.
[4] S. Croci, A. Pecheur, J.L. Autran, A. Vedda, F. Caccavale, M. Martini, G. Spinilo, J. Vac. Sci. Technol. A 19 (2001) 2670.
[5] D. Korzec, D. Theirich, F. Werner, K. Traub, J. Engemann, Surf. Coat. Technol. 74–75 (1995) 67.
[6] S.C. Deshmukh, E.S. Aydil, Appl. Phys. Lett. 65 (1994) 3185.
[7] Y. Inoue, O. Takai, Thin Solid Films 341 (1999) 47.
[8] F. Nicolazo, A. Goullet, A. Granier, C. Vallee, G. Turban, B. Grolleau, Surf. Coat. Technol. 98 (1998) 1578.

[9] K. Aumaille, A. Granier, M. Schmidt, B. Grolleau, C. Vallee, G. Turban, Plasma Sources Sci. Technol. 9 (2000) 331.
[10] S.C. Deshmukh, E.S. Aydil, J. Vac. Sci. Technol. B 14 (1996) 738.
[11] S.B. Bang, T.H. Chung, Y. Kim, Thin Solid Films 444 (2003) 125.
[12] S.B. Bang, T.H. Chung, Y. Kim, M.S. Kang, J.K. Kim, J. Phys. D: Appl. Phys. 37 (2004) 1679.
[13] M.S. Kang, T.H. Chung, Y. Kim, Thin Solid Films 506–507 (2006) 45.
[14] C.J. Chung, T.H. Chung, M.S. Kang, Y. Kim, J. Korean Phys. Soc. 49 (2006) 162.
[15] B.O. Cho, S. Lao, L. Sha, J.P. Chang, J. Vac. Sci. Technol. A 19 (2001) 2751.
[16] A. Granier, C. Vallee, A. Goullet, K. Aumaille, G. Turban, J. Vac. Sci. Technol. A 17 (1999) 2470.
[17] G.B. Raupp, T.S. Cale, H.P.W. Hey, J. Vac. Sci. Technol. B 10 (1992) 37.
[18] C. Vallee, A. Granier, K. Aumaille, C. Cardinaud, A. Goullet, N. Coulon, G. Turban, Appl. Surf. Sci. A 138–139 (1999) 57.
[19] J.A. Theil, J.G. Brace, R.W. Knoll, J. Vac. Sci. Technol. A 12 (1994) 1365.
[20] N. Benissad, C. Boisse-Laporte, C. Vallee, A. Granier, A. Goullet, Surf. Coat. Technol. 116–119 (1999) 868.
[21] J.K. Choi, D.H. Kim, J. Lee, J.B. Yoo, Surf. Coat. Technol. 131 (2000) 136.
[22] C. Vallee, A. Goullet, F. Nicolazo, A. Granier, G. Turban, J. Non-Cryst. Solids 216 (1997) 48.
[23] A. Goullet, C. Vallee, A. Granier, G. Turban, J. Vac. Sci. Technol. A 18 (2000) 2452.
[24] R. Mota, D. Galvao, S.F. Durrant, M. Moraes, S. Dantas, M. Cantao, Thin Solid Films 270 (1995) 109.
[25] Luis da Silva Zambom, P. Verdonck, Thin Solid Films 515 (2006) 596.
[26] C. Rau, W. Kulish, Thin Solid Films 249 (1994) 28.
[27] C.S. Pai, C.P. Chang, J. Appl. Phys. 68 (1990) 793.
[28] Y. Inoue, H. Sugimura, O. Takai, Thin Solid Films 345 (1999) 90.
[29] A.D. Nara, H. Itoh, Jpn. J. Appl. Phys. 36 (1997) 1477.
[30] D.V. Tsu, G. Lucovsky, M.J. Mantini, J. Vac. Sci. Technol. A 5 (1987) 1999.
[31] A.M. Wrobel, M.R. Wertheimer, Plasma-polymerized organosilicons and organometallics, in: R. d'Agostino (Ed.), Plasma Treatment and Etching of Polymers, Academic Press, Boston, 1990.
[32] L. Torrison, J. Tolle, J. Kouvetakis, S.K. Dey, D. Gu, J. Non-Cryst. Solids 288 (2001) 88.
[33] J. Viard, E. Beche, D. Perernau, R. Berjoan, J. Durand, J. Eur. Ceramic Soc. 17 (1997) 2025.
[34] P.G. Pai, S.S. Chao, Y. Takagi, J. Vac. Sci. Technol. A 4 (1986) 689.
[35] A. Yanguas-Gi, J. Cotrino, A.R. Gonzalez-Elipe, J. Phys. D: Appl. Phys. 40 (2007) 3411.
[36] K. Li, O. Gabriel, J. Meichsner, J. Phys. D: Appl. Phys. 37 (2004) 588.
[37] H.U. Kim, S.W. Rhee, J. Mater. Sci.: Mater. Electron. 11 (2000) 579.
[38] E.H. Nicollian, J.R. Brews, MOS physics and Technology, Wiley, New York, 1982.
[39] C. Yi, S.W. Rhee, J. Vac. Sci. Technol. A 20 (2002) 398.